

## Graphene modelocked VECSELS

C.A. Zaugg<sup>1\*</sup>, V.J. Wittwer<sup>2</sup>, Z. Sun<sup>2</sup>, D. Popa<sup>2</sup>, S. Milana<sup>2</sup>, T.S. Kulmala<sup>2</sup>, R.S. Sundaram<sup>2</sup>,  
M. Mangold<sup>1</sup>, M. Golling<sup>1</sup>, Y. Lee<sup>3</sup>, J.H. Ahn<sup>3</sup>, A.C. Ferrari<sup>2</sup> and U. Keller<sup>1</sup>

<sup>1</sup>Department of Physics, Institute for Quantum Electronics, ETH Zürich, 8093 Zürich, Switzerland

<sup>2</sup>Cambridge Graphene Centre, University of Cambridge, Cambridge CB3 0FA, UK

<sup>3</sup>School of Electrical & Electronic Engineering, Yonsei University, Seoul 120-749 and SKKU  
Advanced Institute of Nanotechnology, Sungkyunkwan University, Suwon, 440-746, Korea

### ABSTRACT

In the past decade, passively modelocked optically pumped vertical external cavity surface emitting lasers (OP-VECSELS), sometimes referred to as semiconductor disk lasers (OP-SDLs), impressively demonstrated the potential for generating femtosecond pulses at multi-Watt average output powers with gigahertz repetition rates. Passive modelocking with a semiconductor saturable absorber mirror (SESAM) is well established and offers many advantages such as a flexible design of the parameters and low non-saturable losses.

Recently, graphene has emerged as an attractive wavelength-independent alternative saturable absorber for passive modelocking in various lasers such as fiber or solid-state bulk lasers because of its unique optical properties. Here, we present and discuss the modelocked VECSELS using graphene saturable absorbers. The broadband absorption due to the linear dispersion of the Dirac electrons in graphene makes this absorber interesting for wavelength tunable ultrafast VECSELS. Such widely tunable modelocked sources are in particularly interesting for bio-medical imaging applications.

We present a straightforward approach to design the optical properties of single layer graphene saturable absorber mirrors (GSAMs) suitable for passive modelocking of VECSELS. We demonstrate sub-500 fs pulses from a GSAM modelocked VECSEL. The potential for broadband wavelength tuning is confirmed by covering 46 nm in modelocked operation using three different VECSEL chips and up to 21 nm tuning in pulsed operation is achieved with one single gain chip. A linear and nonlinear optical characterization of different GSAMs with different absorption properties is discussed and can be compared to SESAMs.

Mode-locked lasers, Semiconductor lasers, Vertical emitting lasers, Nanomaterials, Nonlinear optical materials, Tunable lasers.

\*zauggc@phys.ethz.ch; phone +41 44 633 35 78; fax 41 44 633 10 59; [www.ulp.ethz.ch](http://www.ulp.ethz.ch)

## 1. INTRODUCTION

Modelocked ultrafast lasers play an important role in various technologies, from optical communications [1] to medical applications [2] and material processing in industry [3]. Ultrafast vertical-external-cavity surface-emitting lasers (VECSELs)[4], also known as semiconductor disk lasers (SDLs) [5] or optically pumped semiconductor lasers (OPSLs) [5], are excellent pulsed sources for different applications, such as multi-photon imaging [2], optical data communications [5], supercontinuum generation [6] and ultra-compact stabilized frequency combs [4, 5]. A VECSEL, in contrast to a vertical-cavity surface-emitting laser (VCSEL) [7], consists of an external cavity, formed by an output coupler and high-reflection mirrors, with typical cavity dimensions of some cm down to a few mm [4, 8]. The gain chip contains a highly reflective bottom section, an active semiconductor gain section, and an anti-reflective top layer [4, 5, 8]. The VECSEL has been passively modelocked with a semiconductor saturable absorber mirror (SESAM)[9, 10]. VECSELs combine the advantages of semiconductor lasers, such as compact footprint (down to  $\sim 3$  mm cavity [11]), with those of SESAM modelocked diode-pumped solid-state lasers[8], such as low timing jitter [12], excellent beam quality [13], high average [13, 14] and peak power [6, 15].

SESAM offer advantages such as an excellent ratio of saturable to non-saturable losses [16] (e.g. 50:1 [17]) and a high damage threshold ( $>0.21$  J/cm<sup>2</sup>) [17]. However, the bandwidth of the SESAMs tends to be more limited but in the past for solid-state lasers was extended with either absorber bandgap engineering [18] and the underlying standard semiconductor Bragg mirror was extended with novel material growth [19, 20] or by replacing that mirror with a metal mirror [21]. None of these techniques have been used for SESAM modelocked VECSELs. Thus to date, the broadest tuning range of VECSELs mode-locked with SESAMs was 13.7 nm [22]) and have a fast recovery time ranging from hundreds of fs [23] to tens of ps [17]. Graphene saturable absorbers, on the other hand, can easily provide a very broad absorption bandwidth [24-26], due to the gapless linear dispersion of the Dirac electrons, and ultrafast absorber recovery dynamics ( $<100$  fs) [27, 28]. Furthermore, large-area (compared to a typical laser spot), high quality, single layer graphene (SLG) can be easily grown [29] and integrated in a variety of lasers [24, 30]. Due to its low-cost fabrication and assembly [24, 31, 32], graphene based saturable absorbers have emerged as a promising saturable absorber (SA) for ultrafast pulse generation.

The unsaturated loss of a typical intracavity transmission device based on single layer graphene (SLG) is typically  $\sim 2 \times 2.3\%$  (the factor 2 accounting for the double-pass per round-trip) for the most common linear cavities [33, 34]. While this allows to use SLG as saturable absorbers to mode-lock a variety of lasers, such as fiber [31, 32], solid-state [24, 34] and waveguide [35] lasers, it poses serious limitations for VECSELs [4]. These lasers typically require a saturable absorber with  $<3\%$  unsaturated losses [28] because the small-signal gain (i.e. the optical gain for a low-intensity signal where no saturation occurs during amplification) of VECSELs suitable for modelocking is only about 3% to 5% [36]. Thus, inserting a typical SLG-based device (e.g. SLG on a quartz substrate as described in Ref. [34]) introduces too much loss of about  $\approx 4.6\%$  for a double-pass per cavity round-trip and therefore prevents the VECSEL to even reach lasing threshold.

To realize VECSEL modelocking with graphene it is thus crucial to reduce the losses per cavity roundtrip to  $<3\%$  (i.e.  $<1.5\%$  for single pass) while maintaining high (in the range of 0.5- 2% [5]) modulation depth over a spectral range wide enough to have a sufficient modulation for the self-starting passive modelocking of broadband VECSELs. Different methods can be used to reduce the absorption in graphene: Doping [26, 37] or gating [38] can decrease the absorption over a broad spectral range by Pauli blocking [26, 34]. However, it is challenging to precisely control the doping processes and gating usually needs extra electrical contacts and drivers, which increase the complexity of the system.

Here, as published already in [39] we change the absorption by controlling the electric field intensity in SLG on a high reflection mirror [39]. The resulting SLG-based saturable absorber mirrors (GSAMs) have an unsaturated loss adjustable from 0 up to 10% and a modulation depth up to 5%. These GSAMs we have successfully mode-locked VECSELs and benefited from the broadband properties of graphene, demonstrating the widest wavelength-tuning range reported in VECSELs so far. The paper is based on the more detailed report on the GSAM characterization and GSAM modelocked VECSEL, recently published in [39].

## 2. EXPERIMENTAL SETUP

We control the absorption of the graphene as follows: The waves incoming to and reflected from a distributed Bragg reflector (DBR) form a standing wave beyond the mirror surface. The field intensity enhancement at a distance  $z$  from the mirror surface, is [16, 37]:

$$\xi(z) = 4 \sin^2\left(\frac{2\pi n_{\text{air}} z}{\lambda}\right),$$

where  $n_{\text{air}}$  is the refractive index of air and  $\lambda$  is the wavelength. If the medium between the mirror surface of the mirror and the position  $z$  is fused silica ( $\text{SiO}_2$ ), the field intensity enhancement can be calculated to [40]:

$$\xi_{\text{abs}}(d_{\text{SiO}_2}) \approx \frac{4}{1 + n_{\text{SiO}_2}^2 \cot^2\left(\frac{2\pi n_{\text{SiO}_2} d_{\text{SiO}_2}}{\lambda}\right)},$$

where  $n_{\text{SiO}_2}$  is the refractive index of  $\text{SiO}_2$  and  $d_{\text{SiO}_2}$  is the thickness of the spacer layer on top of the mirror. Thus, the single layer graphene (SLG) absorption can be controlled by changing the thickness of the layer below the SLG. The absorption of the SLG becomes  $A = \alpha \xi_{\text{abs}}$ , where  $\alpha \approx 2.3\%$  is the absorption of an undoped and suspended SLG [25], and  $\xi_{\text{abs}}$  is the field intensity enhancement at the position of the absorber. For instance, placing a SLG directly onto the mirror surface ( $z=0$  nm) we get  $\xi_{\text{abs}}=0$  and expect no absorption because of destructive interference between incoming and reflected waves. If SLG is placed at a  $\lambda/4$  distance, where there is a peak of the standing wave, we have  $z=\lambda/4$  and  $\xi_{\text{abs}}=4$ . Therefore, its absorption will increase to 400% (i.e.  $4 \times 2.3\% \approx 9.2\%$ ) due to constructive interference.

For this study [39], we fabricated four GSAMs with different optical distances by coating the mirror with: 0,  $\lambda/12$   $\text{SiO}_2$ ,  $\lambda/8$   $\text{SiO}_2$  and  $\lambda/4$   $\text{SiO}_2$ . We use anti-resonant distributed Bragg reflectors (DBRs) [16] as high-reflection mirrors. These typically consist of a stack of multiple layers with alternating high and low refractive index [16], each with an optical thickness of a quarter of the design wavelength. The partial reflections at the layer interfaces can interfere constructively resulting in high reflection ( $\sim 100\%$  [16]). Our 30-pair anti-resonant AlAs/GaAs (81.1 nm/67.85 nm) DBRs are grown on a 600  $\mu\text{m}$  thick GaAs substrate by molecular beam epitaxy (MBE, VEECO GEN III) [39]. They are designed to give a node of the standing wave at the surface of the top layer (anti-resonance), with reflectivity  $>99.997\%$  at 960 nm (our VECSEL's wavelength). Subsequently, the wafer is cleaved into  $1 \times 1$   $\text{cm}^2$  pieces and then coated by plasma enhanced chemical vapor deposited (Oxford Instruments PECVD 80+)  $\text{SiO}_2$  with different thickness ( $d_{\text{SiO}_2}$ ): 0,  $\lambda/12$ ,  $\lambda/8$  and  $\lambda/4$ , i.e. 0, 55, 83 and 165 nm. This gives a field intensity enhancement  $\xi_{\text{abs}}$  of 0, 0.5, 1.3 and 4, respectively. The layer thickness of the  $\text{SiO}_2$  is measured on reference Si samples with an ellipsometer. Figures 1(a)–1(d) plot schematics of the DBR. SLG is then grown by CVD [24, 41] and transferred onto the mirrors according to [24, 34].

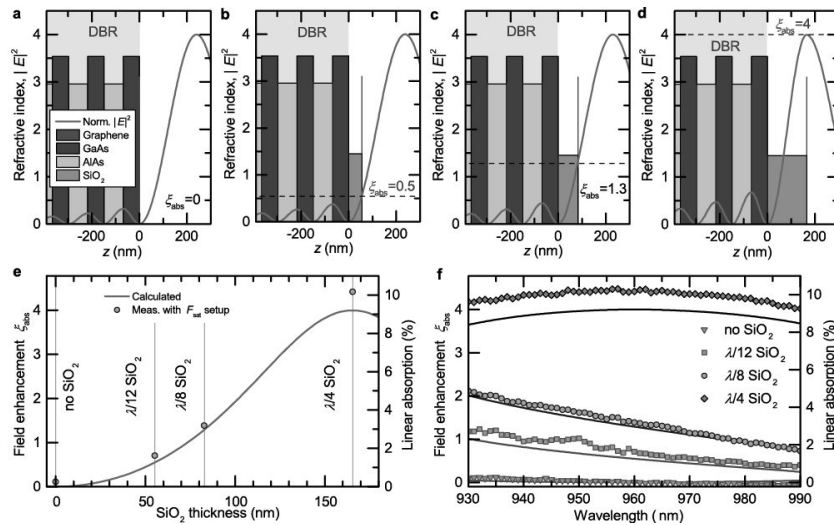


Fig. 1. Zoom of the pairs of the mirror designs with (a) no  $\text{SiO}_2$ , (b)  $\lambda/12$  (55nm)  $\text{SiO}_2$ , (c)  $\lambda/8$  (83nm)  $\text{SiO}_2$  and (d)  $\lambda/4$  (165nm)  $\text{SiO}_2$ . The grey curve represents the normalized standing electric field intensity resulting from the refractive index profile, as a function of the vertical distance from the mirror, for the design wavelength  $\lambda = 960$  nm. A SLG is placed as the last layer. (e) (right axis) linear absorption and (left axis) field intensity enhancement at the SLG location corresponding to the DBRs without  $\text{SiO}_2$  ( $\xi_{\text{abs}}=0$ ), a  $\lambda/12$  layer of  $\text{SiO}_2$  ( $\xi_{\text{abs}}=0.5$ ), a  $\lambda/8$  layer ( $\xi_{\text{abs}}=1.3$ ) and a  $\lambda/4$  layer ( $\xi_{\text{abs}}=4$ ). (f) (lines) calculated and (dots) experimental  $\xi_{\text{abs}}$  and absorption of the four designs as a function of wavelength. Figures from [39].

### 3. ABSORPTION CHARACTERIZATION

The linear unsaturated absorption of our four GSAMs at 960 nm, measured with a high-precision (0.05% resolution) reflectivity setup [42] is plotted in Fig.1(e). Our devices have  $A=0.25\%$ ,  $1.6\%$ ,  $3.2\%$  and  $10\%$  at 960 nm, in agreement with calculations. The field intensity enhancement calculated as a function of the wavelength compared to experiments is shown in Fig. 1(f). This further validates the results [39].

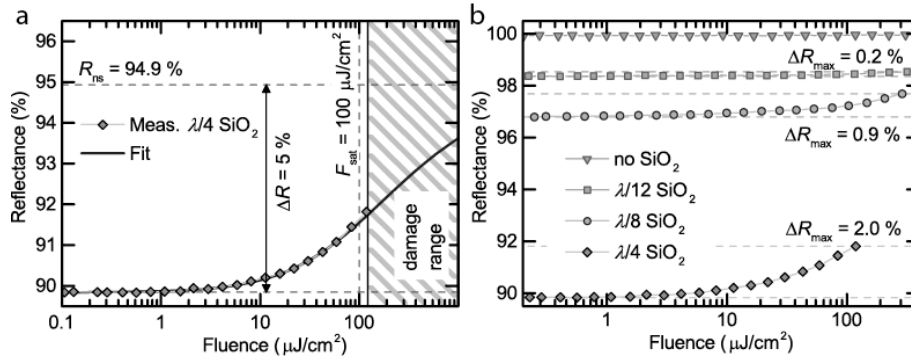


Fig. 2.: (a) Fluence dependent reflectivity measurement of the  $\lambda/4$  SiO<sub>2</sub> sample (square markers) and fit assuming a 5% saturable and 5.1% non-saturable absorption (line), resulting in a saturation fluence of  $100 \mu\text{J}/\text{cm}^2$ . (b) Non-linear reflectivity of all GSAMs. Figures from [39].

Furthermore, we characterized the GSAM's reflectivities as a function of input light fluence ( $\text{J}/\text{cm}^2$ ) using the high-precision reflectivity setup described in [42]. A Kerr-lens mode-locked Ti:Sapphire laser (Tsunami, Spectra-Physics) is used as a probe laser, with 100 fs pulse duration at a 80 MHz repetition rate, with  $\sim 740$  mW average power at 960 nm. The fluence-dependent reflectivity measurements (non-linear reflectivity) show an increase in reflectivity with the fluence as expected from a SA (Fig. 2(d)). The maximum changes in reflectivity for  $\lambda/12$ ,  $\lambda/8$  and  $\lambda/4$  devices are 0.2%, 0.9% and 2%. The measurement for the  $\lambda/4$  SiO<sub>2</sub> device (i.e. the sample with  $\xi=4$  at the graphene position) is shown in Fig. 2(c). We estimate a saturation fluence  $F_{\text{sat}} \sim 100 \mu\text{J}/\text{cm}^2$  (corresponding to a peak intensity  $I_{\text{peak}} \sim 1.0 \text{ GW}/\text{cm}^2$ ) as extracted by fitting the non-linear reflectivity of a fast SA (i.e. where the absorber recovery time is faster than the probe pulse duration) [37] to the data in Fig. 2(c). The estimated modulation depth is  $\sim 5\%$ , 2.7 times larger than that reported for SLG on quartz [33]. When a higher input fluence ( $>120 \mu\text{J}/\text{cm}^2$  ( $4 \text{ GW}/\text{cm}^2$ )) is used, the GSAM reflectivity starts to increase permanently, indicating degradation. The  $F_{\text{sat}}$  of the  $\lambda/8$  sample is estimated as  $\sim 200 \mu\text{J}/\text{cm}^2$ , higher than the  $\lambda/4$  sample, because the smaller field intensity enhancement at the absorber makes the device saturate at a higher fluence. In this case, degradation also starts at higher fluence ( $>300 \mu\text{J}/\text{cm}^2$ ). In SLG, the non-equilibrium (non-thermal) distribution of electrons in conduction band and holes in valence band created by an ultrafast pulse relaxes, eventually reaching thermal equilibrium with the lattice, due to various processes [27, 28], including carrier-carrier and carrier-phonon scattering, as well as radiative electron-hole recombination (non-linear photoluminescence [24, 43, 44]). In the sub-ps time-frame two main processes occur: first, the initial peak produced by the pump laser broadens, due to carrier-carrier collisions, converging towards a hot Fermi-Dirac shape on an ultrashort time scale  $<100$  fs [27, 28]. On a longer timescale, optical phonon emission [45] drives a cooling in which the Fermi Dirac distribution shifts towards the Dirac point [27, 28, 46].

### 4. MODELOCKING RESULTS

For VECSEL modelocking we select the  $\lambda/8$  GSAM because it offers suitable linear loss ( $<3\%$ ) [39]. This device also provides a larger modulation depth ( $>0.9\%$ ) compared to the  $\lambda/12$  GSAM. The laser cavity configuration is sketched in Fig. 3(a), with a picture in Fig. 3(b). The resonator mode and pump spot radius on the gain chip are  $150 \mu\text{m}$ . In order to achieve a sufficient intensity to saturate the GSAM, we implement a beam waist  $\sim 30 \mu\text{m}$  on the absorber using a concave folding mirror with a 20 mm radius of curvature. A picture of the  $\lambda/8$ -GSAM is shown in Fig. 3(c).

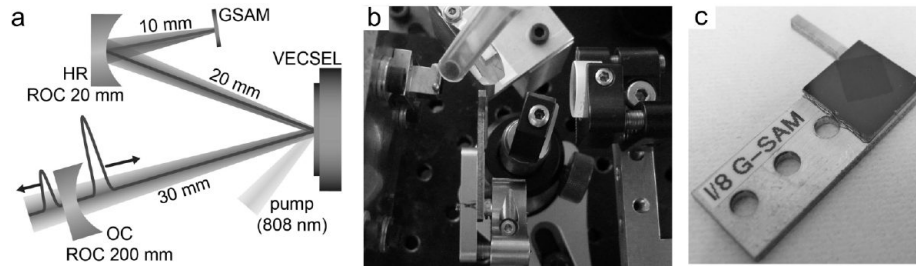


Fig. 3. (a) VECSEL setup. OC: output coupler mirror. HR: high reflective mirror. GSAM: graphene saturable absorber. The gain chip is placed as a folding mirror and pumped under a 45° angle. The cavity length is 6 cm. (b) Picture of the laser setup. (c) Picture of the  $\lambda/8$  GSAM. The SLG can be seen as a shaded area, since the 83 nm SiO<sub>2</sub> thickness gives a high optical contrast in the visible range [42]. Figures from [39].

We use three different VECSEL gain chips: Two QW VECSELs emitting at  $\sim 940$  and  $970$  nm are grown by metal-organic vapor phase epitaxy (MOVPE, AIXTRON AIX 200/4) as described in [47]. A QD VECSEL with an emission wavelength  $\sim 950$  nm is grown by MBE as described in [23]. Instead of 9 QD layers placed in 7 subsequent anti-nodes of the electric field as in [47], our gain chip has  $2 \times 9$  QD layers placed in the first anti-node, whereas no QDs are placed in the 6th anti-node, so to balance the stronger excitation due to higher absorption of the pump light around the first anti-nodes. All gain structures are grown in reverse order, and subsequently processed on a diamond heat sink grown by CVD as described in [48]. The pump laser is coupled into a 200  $\mu\text{m}$  fiber.

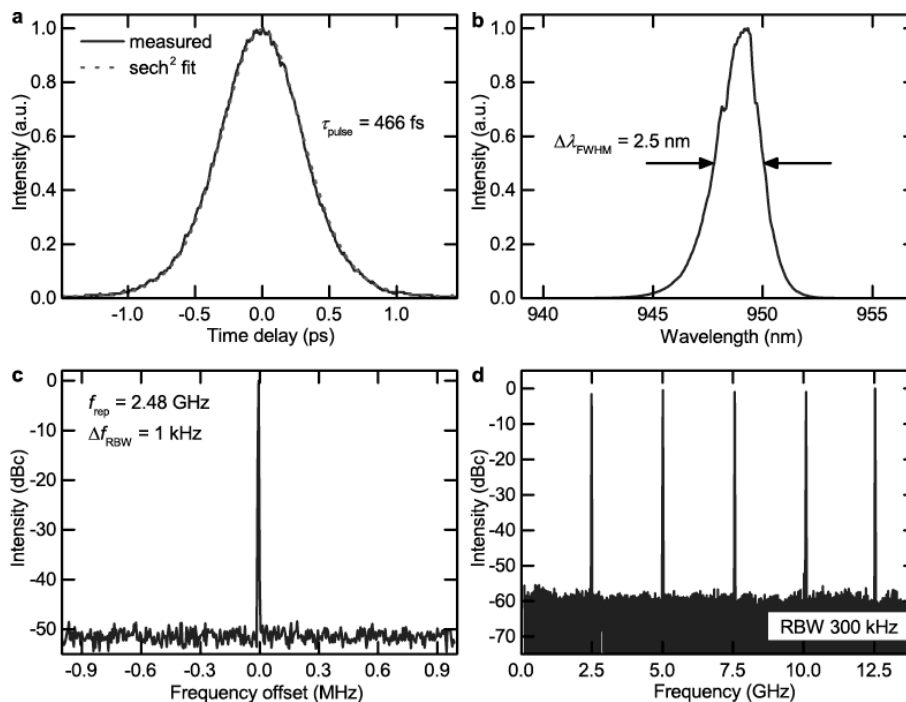


Fig. 4. Femtosecond pulses from a GSAM modelocked VECSEL: (a) autocorrelation measurement with fit to the autocorrelation of a  $\text{sech}^2$ -pulse reveals a pulse duration of 466 fs; (b) optical spectrum centered at  $\sim 949$  nm; (c) narrow and (d) wide span RF spectrum indicating a repetition rate of 2.5 GHz. Figures from [39].

Using the gain chip optimized for  $\sim 950$  nm, we obtain stable modelocking with a pulse duration of 466 fs, measured with an intensity autocorrelator (Femtochrome FR103XL) as shown in Fig. 4(a). The spectrum is centered at  $\sim 949$  nm with  $\text{FWHM} = 2.5$  nm, Fig. 4(b), as analyzed with an optical spectrum analyzer (HP 70952). Note that the field intensity enhancement of our  $\lambda/8$  GSAM is  $\xi_{\text{abs}} = 1.5$  at 949 nm compared to 1.3 at 960 nm, see Fig. 1(f). The pulse repetition rate is 2.5 GHz, detected with a fast photodiode (New Focus 1434) and measured with a microwave spectrum analyzer (MSA, HP 70952), see Fig. 4(c) and 4(d), one order of magnitude higher than previous fiber [30, 32] and solid-state [30,

34] lasers mode-locked by graphene, due to the compactness of our VECSEL design. The time-bandwidth product is 0.353, 1.1 times larger than what expected for transform-limited  $\text{sech}^2$  pulses, indicating that the output pulses are slightly chirped. The average output power is 12.5 mW, with a 0.2% output coupling (OC) transmission. Higher power up to 26 mW with 2 ps pulses is also achieved using a 0.5% OC transmission. We calculate the input pulse fluence on the GSAM as  $\sim 125 \mu\text{J}/\text{cm}^2$ , corresponding to a reflectivity modulation of  $\sim 0.55\%$ , according to Fig. 2(a). We did not observe any degradation of the GSAM for several hours operation [39].

In order to verify the broadband operation of our GSAM, we also perform a wavelength tuning study using the VECSELS described above. We use a  $\sim 10$  cm cavity at 1.5 GHz, with various OC transmission rates and gain chips to fully test our GSAMs. A Fabry-Pérot fused silica etalon (20  $\mu\text{m}$  thick) is used for wavelength tuning. In order to optimize the output power at a given emission wavelength, the gain chip heat sink temperature is adjusted between  $-20$  and  $+20^\circ\text{C}$ . Modelocked operation is obtained in a range from 935 to 981 nm (46 nm), with pulse durations up to 8 ps as shown in Fig. 5(d). Figures 5(a) and 5(b) show the pulse duration and average output power for different emission wavelengths. A maximum tuning range of 21 nm with a single VECSEL gain chip is achieved with the 970 nm QW VECSEL, Fig. 5(c). This is larger than previously reported with any SESAM mode-locked VECSEL [22].

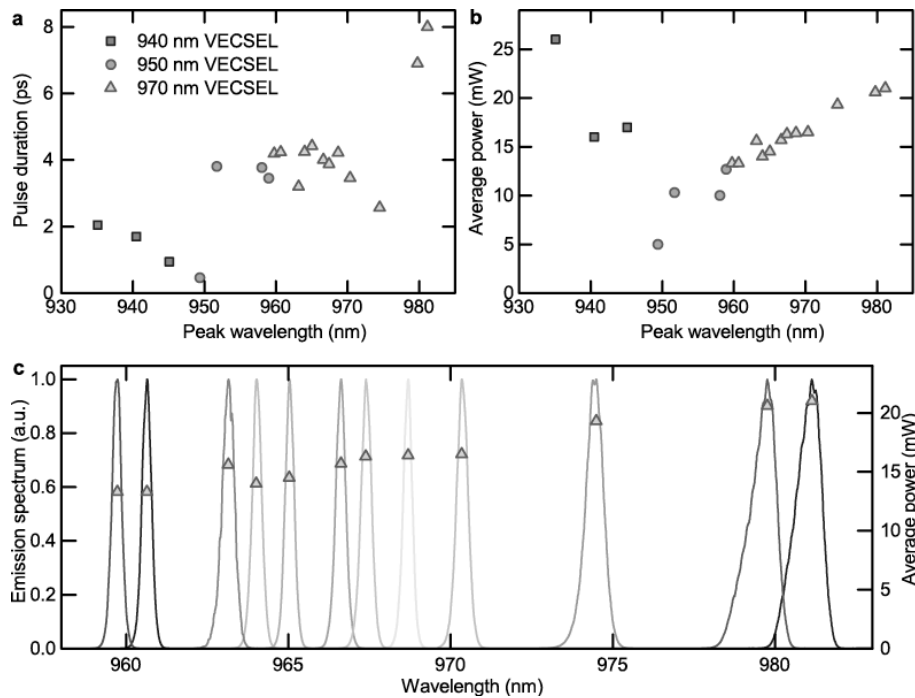


Fig. 5. Tuning results. Modelocking with the  $\lambda/8$  GSAM in VECSELS optimized for different emission wavelengths. An intra-cavity etalon is used, except for the two points at 935 and 949 nm. (a) Pulse duration and (b) average output power at different emission wavelengths. (c) Emission spectra for the 970 nm-VECSEL and average output power. Figures from [39].

## 5. CONCLUSION

We demonstrated a versatile approach to engineer the absorption of graphene saturable absorber mirrors (GSAMs) in the 0-10% range [39]. Accordingly, the saturation fluence can be adjusted with the field intensity enhancement. We mode-locked VECSELS with a series of different gain chips over a 46 nm wavelength range (from 935 to 981 nm) with repetition rates up to 2.48 GHz, and 466 fs pulse duration. At this point the average power was limited by the onset of damage before the GSAM has been fully saturated. This results in a higher cavity insertion loss which is more severe for high-Q cavities. Further improvements in GSAM production, however, should address this issue. Thus, this approach can lead to novel broadband ultrafast light sources to meet the wavelength range, repetition rate and pulse duration requirements for various applications (e.g. metrology, spectroscopy and data-communication).

## ACKNOWLEDGMENTS

We thank Prof. T. Südmeyer for useful discussions. We acknowledge funding from a Royal Society Wolfson Research Merit Award, the European Research Council Grants NANOPOTS, Hetero2D, EU grants RODIN, GENIUS, MEM4WIN, CareRAMM, and Graphene Flagship (contract no. NECT-ICT-604391), EPSRC grants EP/K01711X/1, EP/K017144/1, EP/G042357/1, Nokia Research Centre, Emmanuel College, Cambridge, the FIRST clean room facility of ETH, the Swiss National Science Foundation (SNSF) and the Swiss Confederation Program Nano-Tera.ch, which was scientifically evaluated by the SNSF.

## REFERENCES

- [1] D. Hillerkuss, R. Schmogrow, T. Schellinger, M. Jordan, M. Winter, G. Huber, T. Vallaitis, R. Bonk, P. Kleinow, F. Frey, M. Roeger, S. Koenig, A. Ludwig, A. Marculescu, J. Li, M. Hoh, M. Dreschmann, J. Meyer, S. Ben Ezra, N. Narkiss, B. Nebendahl, F. Parmigiani, P. Petropoulos, B. Resan, A. Oehler, K. Weingarten, T. Ellermeyer, J. Lutz, M. Moeller, M. Huebner, J. Becker, C. Koos, W. Freude, and J. Leuthold, "26 Tbit s<sup>-1</sup> line-rate super-channel transmission utilizing all-optical fast Fourier transform processing," *Nat Photon* **5**, 364-371 (2011).
- [2] R. Aviles-Espinosa, G. Filippidis, C. Hamilton, G. Malcolm, K. J. Weingarten, T. Südmeyer, Y. Barbarin, U. Keller, S. I. C. O. Santos, D. Artigas, and P. Loza-Alvarez, "Compact ultrafast semiconductor disk laser: targeting GFP based nonlinear applications in living organisms," *Biomed. Opt. Express* **2**, 739-747 (2011).
- [3] M. E. Fermann, A. Galvanauskas, and G. Sucha, *Ultrafast lasers: technology and applications* (CRC Press, 2003).
- [4] U. Keller, and A. C. Tropper, "Passively modelocked surface-emitting semiconductor lasers," *Phys. Rep.* **429**, 67-120 (2006).
- [5] T. Südmeyer, D. J. H. C. Maas, and U. Keller, "Mode-Locked Semiconductor Disk Lasers," in *Semiconductor Disk Lasers*, O. G. Okhotnikov, ed. (Wiley-VCH Verlag GmbH & Co. KGaA, 2010), pp. 213-261.
- [6] K. G. Wilcox, A. C. Tropper, H. E. Beere, D. A. Ritchie, B. Kunert, B. Heinen, and W. Stolz, "4.35 kW peak power femtosecond pulse mode-locked VECSEL for supercontinuum generation," *Opt. Express* **21**, 1599-1605 (2013).
- [7] J. L. Jewell, J. P. Harbison, A. Scherer, Y. H. Lee, and L. T. Florez, "Vertical-cavity surface-emitting lasers: Design, growth, fabrication, characterization," *Quantum Electronics, IEEE Journal of* **27**, 1332-1346 (1991).
- [8] U. Keller, "Recent developments in compact ultrafast lasers," *Nature* **424**, 831-838 (2003).
- [9] U. Keller, D. A. B. Miller, G. D. Boyd, T. H. Chiu, J. F. Ferguson, and M. T. Asom, "Solid-state low-loss intracavity saturable absorber for Nd:YLF lasers: an antiresonant semiconductor Fabry-Perot saturable absorber," *Opt. Lett.* **17**, 505-507 (1992).
- [10] U. Keller, K. J. Weingarten, F. X. Kärtner, D. Kopf, B. Braun, I. D. Jung, R. Fluck, C. Hönninger, N. Matuschek, and J. Aus der Au, "Semiconductor saturable absorber mirrors (SESAMs) for femtosecond to nanosecond pulse generation in solid-state lasers," *IEEE J. Sel. Top. Quantum Electron.* **2**, 435-453 (1996).
- [11] D. Lorensen, D. J. H. C. Maas, H. J. Unold, A.-R. Bellancourt, B. Rudin, E. Gini, D. Ebling, and U. Keller, "50-GHz passively mode-locked surface-emitting semiconductor laser with 100 mW average output power," *IEEE J. Quantum Electron.* **42**, 838-847 (2006).
- [12] V. J. Wittwer, C. A. Zaugg, W. P. Pallmann, A. E. H. Oehler, B. Rudin, M. Hoffmann, M. Golling, Y. Barbarin, T. Südmeyer, and U. Keller, "Timing Jitter Characterization of a Free-Running SESAM Mode-locked VECSEL," *Photonics Journal, IEEE* **3**, 658-664 (2011).
- [13] B. Rudin, V. J. Wittwer, D. J. H. C. Maas, M. Hoffmann, O. D. Sieber, Y. Barbarin, M. Golling, T. Südmeyer, and U. Keller, "High-power MIXSEL: an integrated ultrafast semiconductor laser with 6.4 W average power," *Opt. Express* **18**, 27582-27588 (2010).
- [14] B. Heinen, T. L. Wang, M. Sparenberg, A. Weber, B. Kunert, J. Hader, S. W. Koch, J. V. Moloney, M. Koch, and W. Stolz, "106 W continuous-wave output power from vertical-external-cavity surface-emitting laser," *Electronics Letters* **48**, 516-517 (2012).
- [15] M. Scheller, T. L. Wang, B. Kunert, W. Stolz, S. W. Koch, and J. V. Moloney, "Passively modelocked VECSEL emitting 682 fs pulses with 5.1W of average output power," *Electronics Letters* **48**, 588-589 (2012).
- [16] G. J. Spühler, K. J. Weingarten, R. Grange, L. Krainer, M. Haiml, V. Liverini, M. Golling, S. Schon, and U. Keller, "Semiconductor saturable absorber mirror structures with low saturation fluence," *Appl. Phys. B* **81**, 27-32 (2005).
- [17] C. J. Saraceno, C. Schriber, M. Mangold, M. Hoffmann, O. H. Heckl, C. R. E. Baer, M. Golling, T. Südmeyer, and U. Keller, "SESAMs for high-power oscillators: design guidelines and damage thresholds," *IEEE J. Sel. Top. Quantum Electron.* **18**, 29-41 (2012).
- [18] G. R. Jacobovitz-Veselka, M. T. Asom, and U. Keller, "Broadband fast semiconductor saturable absorber," *Opt. Lett.* **17**, 1791-1793 (1992).
- [19] S. Schön, M. Haiml, L. Gallmann, and U. Keller, "Fluoride semiconductor saturable-absorber mirror for ultrashort pulse generation," *Opt. Lett.* **27**, 1845-1847 (2002).
- [20] S. Schön, M. Haiml, L. Gallmann, and U. Keller, "GaAs absorber layer growth for broadband AlGaAs/fluoride SESAMs," *Journal of Crystal Growth* **227**, 172-176 (2001).
- [21] R. Fluck, I. D. Jung, G. Zhang, F. X. Kärtner, and U. Keller, "Broadband saturable absorber for 10-fs pulse generation," *Opt. Lett.* **21**, 743-745 (1996).
- [22] O. J. Morris, K. G. Wilcox, C. R. Head, A. P. Turnbull, P. J. Mosley, A. H. Quarterman, H. J. Khashi, I. Farrer, H. E. Beere, D. A. Ritchie, and A. C. Tropper, "A wavelength tunable 2-ps pulse VECSEL," in *Photonics West*(SPIE, 2012), pp. 824212-824212.
- [23] M. Hoffmann, O. D. Sieber, V. J. Wittwer, I. L. Krestnikov, D. A. Livshits, Y. Barbarin, T. Südmeyer, and U. Keller, "Femtosecond high-power quantum dot vertical external cavity surface emitting laser," *Opt. Express* **19**, 8108-8116 (2011).

- [24] F. Bonaccorso, Z. Sun, T. Hasan, and A. C. Ferrari, "Graphene photonics and optoelectronics," *Nat Photon* **4**, 611-622 (2010).
- [25] R. R. Nair, P. Blake, A. N. Grigorenko, K. S. Novoselov, T. J. Booth, T. Stauber, N. M. R. Peres, and A. K. Geim, "Fine Structure Constant Defines Visual Transparency of Graphene," *Science* **320**, 1308-1308 (2008).
- [26] K. F. Mak, M. Y. Sfeir, Y. Wu, C. H. Lui, J. A. Misewich, and T. F. Heinz, "Measurement of the Optical Conductivity of Graphene," *Physical Review Letters* **101**, 196405 (2008).
- [27] D. Brida, A. Tomadin, C. Manzoni, Y. J. Kim, A. Lombardo, S. Milana, R. R. Nair, K. S. Novoselov, A. C. Ferrari, G. Cerullo, and M. Polini, "Ultrafast collinear scattering and carrier multiplication in graphene," *Nat Commun* **4** (2013).
- [28] A. Tomadin, D. Brida, G. Cerullo, A. C. Ferrari, and M. Polini, "Nonequilibrium dynamics of photoexcited electrons in graphene: Collinear scattering, Auger processes, and the impact of screening," *Physical Review B* **88**, 035430 (2013).
- [29] F. Bonaccorso, A. Lombardo, T. Hasan, Z. Sun, L. Colombo, and A. C. Ferrari, "Production and processing of graphene and 2d crystals," *Materials Today* **15**, 564-589 (2012).
- [30] Z. Sun, T. Hasan, and A. C. Ferrari, "Ultrafast lasers mode-locked by nanotubes and graphene," *Physica E: Low-dimensional Systems and Nanostructures* **44**, 1082-1091 (2012).
- [31] T. Hasan, Z. Sun, F. Wang, F. Bonaccorso, P. H. Tan, A. G. Rozhin, and A. C. Ferrari, "Nanotube-Polymer Composites for Ultrafast Photonics," *Advanced Materials* **21**, 3874-3899 (2009).
- [32] Z. Sun, T. Hasan, F. Torrisi, D. Popa, G. Privitera, F. Wang, F. Bonaccorso, D. M. Basko, and A. C. Ferrari, "Graphene Mode-Locked Ultrafast Laser," *ACS Nano* **4**, 803-810 (2010).
- [33] I. H. Baek, H. W. Lee, S. Bae, B. H. Hong, Y. H. Ahn, D.-I. Yeom, and F. Rotermund, "Efficient Mode-Locking of Sub-70-fs Ti:Sapphire Laser by Graphene Saturable Absorber," *Applied Physics Express* **5**, 032701 (2012).
- [34] A. A. Lagatsky, Z. Sun, T. S. Kulmala, R. S. Sundaram, S. Milana, F. Torrisi, O. L. Antipov, Y. Lee, J. H. Ahn, C. T. A. Brown, W. Sibbett, and A. C. Ferrari, "2 $\mu$ m Solid-State Laser Mode-locked By Single-Layer Graphene," *Applied Physics Letters* **102**, 013113 (2013).
- [35] R. Mary, G. Brown, S. J. Beecher, F. Torrisi, S. Milana, D. Popa, T. Hasan, Z. Sun, E. Lidorikis, S. Ohara, A. C. Ferrari, and A. K. Kar, "1.5 GHz picosecond pulse generation from a monolithic waveguide laser with a graphene-film saturable output coupler," *Opt. Express* **21**, 7943-7950 (2013).
- [36] M. Mangold, V. J. Wittwer, O. D. Sieber, M. Hoffmann, I. L. Krestnikov, D. A. Livshits, M. Golling, T. Südmeyer, and U. Keller, "VECSSEL gain characterization," *Opt. Express* **20**, 4136-4148 (2012).
- [37] C. C. Lee, J. M. Miller, and T. R. Schibli, "Doping-induced changes in the saturable absorption of monolayer graphene," *Applied Physics B* **108**, 129-135 (2012).
- [38] F. Wang, Y. B. Zhang, C. S. Tian, C. Girit, A. Zettl, M. Crommie, and Y. R. Shen, "Gate-variable optical transitions in graphene," *Science* **320**, 206-209 (2008).
- [39] C. A. Zaugg, Z. Sun, V. J. Wittwer, D. Popa, S. Milana, T. S. Kulmala, R. S. Sundaram, M. Mangold, O. D. Sieber, M. Golling, Y. Lee, J. H. Ahn, A. C. Ferrari, and U. Keller, "Ultrafast and widely tuneable vertical-external-cavity surface-emitting laser, mode-locked by a graphene-integrated distributed Bragg reflector," *Opt. Express* **21**, 31548-31559 (2013).
- [40] B. E. A. Saleh, and M. K. Teich, *Fundamentals of Photonics* (John Wiley & Sons, Inc., 2007).
- [41] S. Bae, H. Kim, Y. Lee, X. Xu, J.-S. Park, Y. Zheng, J. Balakrishnan, T. Lei, H. Ri Kim, Y. I. Song, Y.-J. Kim, K. S. Kim, B. Ozyilmaz, J.-H. Ahn, B. H. Hong, and S. Iijima, "Roll-to-roll production of 30-inch graphene films for transparent electrodes," *Nat Nano* **5**, 574-578 (2010).
- [42] D. J. H. C. Maas, B. Rudin, A.-R. Bellancourt, D. Iwaniuk, S. V. Marchese, T. Südmeyer, and U. Keller, "High precision optical characterization of semiconductor saturable absorber mirrors," *Opt. Express* **16**, 7571-7579 (2008).
- [43] W.-T. Liu, S. W. Wu, P. J. Schuck, M. Salmeron, Y. R. Shen, and F. Wang, "Nonlinear broadband photoluminescence of graphene induced by femtosecond laser irradiation," *Physical Review B* **82**, 081408 (2010).
- [44] C. H. Lui, K. F. Mak, J. Shan, and T. F. Heinz, "Ultrafast Photoluminescence from Graphene," *Physical Review Letters* **105**, 127404 (2010).
- [45] M. Lazzeri, S. Piscanec, F. Mauri, A. C. Ferrari, and J. Robertson, "Electron Transport and Hot Phonons in Carbon Nanotubes," *Physical Review Letters* **95**, 236802 (2005).
- [46] E. Malic, T. Winzer, and A. Knorr, "Efficient orientational carrier relaxation in optically excited graphene," *Applied Physics Letters* **101**, 213110 (2012).
- [47] D. Lorenser, H. J. Unold, D. J. H. C. Maas, A. Aschwanden, R. Grange, R. Paschotta, D. Ebling, E. Gini, and U. Keller, "Towards Wafer-Scale Integration of High Repetition Rate Passively Mode-Locked Surface-Emitting Semiconductor Lasers," *Appl. Phys. B* **79**, 927-932 (2004).
- [48] R. Häring, R. Paschotta, A. Aschwanden, E. Gini, F. Morier-Genoud, and U. Keller, "High-power passively mode-locked semiconductor lasers," *IEEE J. Quantum Electron.* **38**, 1268-1275 (2002).